Journal of Inflammation Research

Dovepress
open access to scientific and medical research

Open Access Full Text Article

ORIGINAL RESEARCH

Comprehensive Analysis of SLC35A2 in Pan-Cancer and Validation of Its Role in Breast Cancer

Xiaonan Sun[1], Zhichao Yuan[1], Lu Zhang[1], Min Ren[2], Jing Yang[2], Yidan Xu[1], Jiqing Hao[1]

[1]Department of Oncology, The First Affiliated Hospital of Anhui Medical University, Hefei, Anhui Province, People's Republic of China; [2]Department of Breast Surgery, The First Affiliated Hospital of Anhui Medical University, Hefei, Anhui Province, People's Republic of China

Correspondence: Jiqing Hao, Department of Oncology, The First Affiliated Hospital of Anhui Medical University, Hefei, Anhui Province, 230022, People's Republic of China, Email haojiqing@ahmu.edu.cn

Purpose: Elucidation of the oncogenic role of SLC35A2 in human tumors and the potential function and clinical significance in breast cancer.

Methods: Pan-cancer analysis was performed via various bioinformatics tools to explain the pathogenic role of SLC35A2. A prognostic nomogram was also developed based on the SLC35A2 expression and clinicopathological characteristics in breast cancer patients. In addition, the role of SLC35A2 was validated in breast cancer by in vivo and in vitro experiments.

Results: SLC35A2 expression is increased in 27 tumor types, and its high expression is substantially correlated with poor prognosis in patients with a variety of cancers. Receiver operating characteristic (ROC) curves showed that SLC35A2 expression levels could accurately distinguish most tumor tissues from normal tissues. High SLC35A2 expression was linked to increased immune infiltration in myeloid-derived suppressor cells (MDSC), as well as immune checkpoints, ferroptosis-related genes, tumor mutational burden (TMB), and microsatellite instability (MSI). SLC35A2 may be involved in tumorigenesis by regulating the glycosylation process. Furthermore, multivariate Cox analysis showed that SLC35A2 was an independent prognostic factor for breast cancer. And the nomogram model had good predictive accuracy for the prognosis of breast cancer patients. Meanwhile, cellular experiments demonstrated that knockdown of SLC35A2 could significantly inhibit the proliferation, migration and invasion of breast cancer cells, while increasing the protein level of E-cadherin and decreasing N-cadherin. A nude mouse xenograft model showed that inhibition of SLA35A2 expression could significantly inhibit tumor growth.

Conclusion: SLC35A2 has good diagnostic and prognostic values in multiple cancers and is closely related to tumor immune infiltration. In addition, SLA35A2 as an oncogene in breast cancer may be involved in the progression of epithelial mesenchymal transition (EMT).

Keywords: SLC35A2, pan-cancer, breast cancer, prognostic, tumor microenvironment, EMT

Introduction

SLC35A2 is a member of the solute carrier 35 (SLC35) family and encodes the uridine diphosphate galactose (UDP-Gal). The latter belongs to the nucleotide sugar transporter proteins, which contain 10 transmembrane regions responsible for the transport of UDP-Gal from the cytoplasm to the Golgi lumen and then to the endoplasmic reticulum.[1] SLC35A2 is located on the X chromosome, and its pathogenic variation is related to a rare genetic disease, congenital glycosylation disorder.[2] Most affected individuals have different degrees of nervous system symptoms, with epileptic encephalopathy being the main feature, while others have mental retardation and deformity.[3,4] SLC35A2 regulates glycosylation modifications on the surface of hepatocellular carcinoma cells, produces an aberrant expression of adhesion molecules, and increases hepatocellular carcinoma cell invasion and metastatic capacity, according to recent research.[5] Clinical trials have revealed that high SLC35A2 expression has been linked to poor prognosis in individuals with breast and hepatocellular carcinoma.[6] The investigators found that SLC35A2 has a role in regulating cell cycles using a process-based analysis of SLC35A2 co-expressed genes.[7] SLC35A2 and other adhesion molecules are highly expressed in colon cancer as a result of hypoxia.[8] Furthermore, experiments conducted in vitro revealed that the solute carrier family is associated with cytotoxic drug uptake

Received: 8 May 2023
Accepted: 6 August 2023
Published: 11 August 2023

and cellular activity, and inactivation of the SLC35A2 transporter leads to reduced sensitivity of cancer cells to cisplatin.[9] SLC35A2's role in tumors is still in its exploratory stages, and there is a dearth of pan-cancer proof for its connection with numerous tumor types. Therefore, it is necessary to explore and analyze the comprehensive performance and function of the SLC35A2 gene in pan-cancer.

At present, publicly funded cancer genomics databases are widely used in pan-cancer research. By combining these tools with a variety of genomics analyses, we can understand the mechanisms of tumor occurrence and development more comprehensively and deeply. We examined the SLC35A2 gene across all cancer types utilizing various databases and investigated the role of SLC35A2 in cancer pathogenesis and clinical prognosis. In addition, this study constructed a breast cancer survival prediction model and validated the biological role of SLC35A2 in breast cancer by in vitro and in vivo experiments. The findings of this work help advance understanding of the differential expression of SLC35A2 in all types of cancer, shed light on SLC35A2's potential as a biomarker for prognosis and immunity, and demonstrate SLC35A2's clinical significance and function in breast cancer.

Materials and Methods

Gene Expression

We studied 33 tumor tissues and their adjacent normal tissue in the "Pan-Cancer Analysis" module on the Xiantao website (https://www.xiantaozi.com/). We integrated data from the cancer genome atlas (TCGA) tumor tissues with data from normal tissues in the GTEx database for analysis. Web-based GEPIA2 (http://gepia2.cancer-pku.cn/#index) offers quick and customizable features such as general information, similar genes detection, and differential expression analysis.[10] SLC35A2 expression was analyzed by GEPIA2 in multiple tumor types at different pathological stages. A list of cancer abbreviations is provided in Supplementary Table S1.

Survival Prognosis and Tumor Diagnosis

Using the GEPIA2 "Survival Map" and "Survival Analysis" modules, we were able to obtain the overall survival (OS) and disease-free survival (DFS) graphs of SLC35A2 in pan-cancer. A Kaplan-Meier plot was used to assess the impact of the SLC35A2 gene on cancer survival (http://kmplot.com/analysis/). The database has been compiled from GEO, EGA, and TCGA.[11] According to the median expression value of SLC35A2, we categorized the patients into two groups: low-expression (Cutoff-Low (%): <50) and high-expression (Cutoff-High (%): ≥50). A univariate Cox regression was performed to analyze the survival probability of SLC35A2 on the data in the TCGA database, and a forest plot was drawn. To better understand the diagnostic usefulness of SLC35A2 expression levels in various cancer types, we lastly plotted receiver operating characteristic (ROC) curves.

Immune and Molecular Subtypes

The TISIDB database (http://cis.hku.hk/TISIDB/index.php) is a comprehensive analysis of the tumor immune system website,[12] was utilized to investigate the relationship between SLC35A2 expression and immunological or molecular subtypes of various cancer types.

Tumor Microenvironment (TME)

The relation between SLC35A2 expression and immune infiltration cells in pan-cancer was studied utilizing the "Immune" module of the TIMER2.0 (http://timer.cistrome.org/). The Sanger Box (http://sangerbox.com/index.html) and the Xiantao website were applied to investigate the association between SLC35A2 expression and ferroptosis-related genes, immune checkpoint genes, and biomarkers in the tumor microenvironment. By reviewing prior publications, ferroptosis, and immune checkpoint-related genes were chosen,[13–15] and tumor mutation burden (TMB) and microsatellite instability (MSI) have been identified as TME biomarkers.

Gene Enrichment Analysis

To perform functional enrichment analysis of the protein-protein interaction network, we used the STRING web portal (https://string-db.org/) to retrieve SLC35A2 binding proteins.[16] We identified the top 100 SLC35A2-related target genes from a dataset of all TCGA cancers using the GEPIA2 "Similar Genes Discovery" module. To compare SLC35A2 binding and interacting genes, we employed cross-tabulation analysis with Venn diagrams. In addition, we integrated two data sets to perform the Kyoto Encyclopedia of Genes and Genomes (KEGG) pathway analysis and Gene Ontology (GO) enrichment.

Correlation Analysis of Clinical Factors

All raw data were obtained from the TCGA database. We analyzed the clinicopathological characteristics and logistic regression analysis of SLC35A2 expression. To further assess SLC35A2's prognostic significance in breast cancer patients, we performed a ROC curve and multivariate Cox regression analysis. In a multivariate Cox analysis, a nomogram was established based on independent prognostic factors. The performance of the nomogram was then assessed using calibration plots and the nomogram was quantified using a consistency index (C-index).

Cell Culture

Human breast cancer cell lines MCF7, BT474, MDA-MB-231, and normal breast cells MCF10A were originally purchased from the cell bank of the Chinese Academy of Sciences (Shanghai, China) and provided by the Department of Breast Surgery, The First Affiliated Hospital of Anhui Medical University. The use of the cell lines was approved by the Medical Ethics Committee of the First Affiliated Hospital of Anhui Medical University (approval number: 2023494). MCF7, BT474, and MDA-MB-231 cells were cultured in DMEM (Gibco, USA) supplemented with 10% fetal bovine serum (FBS, Gibco, USA). MCF10A cells were cultured in MCF10A cell-specific medium (Procell, China). The cell cultivation conditions were 37°C with 5% CO_2. Gene Pharma (https://www.genepharma.com/) provided the human target gene SLC35A2 small interfering RNA (siRNA). The sequences are as follows: siSLC35A2-1, F: 5′-GA AGUGCUCAAAGGUCUCATT-3′; R: 5′-UGAGACCUUUGAGCACUUCTT-3′; siSLC35A2-2, F: 5′-GC CUGAAGUACAUAUCCCUTT-3′; R: 5′-AGGGAUAUGUACUUCAGGCTT-3′; siSLC35A2-3, F: 5′-CC ACUUUCCAGGUGACAUATT-3′; R: 5′-UAUGUCACCUGGAAAGUGGTT-3′; siSLC35A2-4, F: 5′-GUUGUCAAGUACGCUGACATT-3′; R: 5′-UGUCAGCGUACUUGACAACTT-3′. MCF7 cells were inoculated in six-well plates, and cells were transfected with GP-transfect-Mate (catalog number G04008; Genepharma) after cell walling.

Real-Time Quantitative PCR (RT-qPCR)

Novoprotein Scientific Inc. provided both the reverse transcription kit (catalog number E047) and the qPCR kit (catalog number E096), and the primers were designed and synthesized by General Biol (Anhui) Co., Ltd. Cells were extracted with the RNA extraction kit (catalog number R4111) based on Magen's instructions. The RNA extracted in the last step was transformed into cDNA by reverse transcription kit, and then Hot-Star Taq was premixed by SYBR, and RT-qPCR was performed on Roche Applied Science Light Cycler 480. Use the following primers: SLC35A2-F, 5′-GAATGGCCTCCATCCCAG-3′; SLC35A2-R, 5′- CCTTTGAGCACTTCCGCCAT-3′; GAPDH processed all results for standardization. The $2^{-\Delta\Delta\ Ct}$ method was used to calculate the gene's relative expression level.

Immunohistochemistry (IHC) and Western Blot

Ten pairs of breast cancer tumor tissue specimens and adjacent normal tissue specimens were provided by the Department of Breast Surgery, The First Affiliated Hospital of Anhui Medical University. Written informed consent was obtained from patients and/or families before surgery. The study was conducted in accordance with the Declaration of Helsinki (revised 2013) and approved by the Medical Ethics Committee of the First Affiliated Hospital of Anhui Medical University (approval number: 5101389). The SLC35A2 antibody (catalog number 13657-1-AP) was purchased from Wuhan San Ying Biotechnology Group Co., Ltd and the E-cadherin (catalog number WL01482) and N-cadherin (catalog number WL01047) antibodies were purchased from Wan lei Co. The expression of SLC35A2 in breast cancer

tissues and adjacent normal samples was detected by IHC, and the levels of SLC35A2 and epithelial-mesenchymal transition (EMT) protein were examined by Western blot. The experiments were repeated thrice.

Cell Counting Kit-8 (CCK-8) Detection

Transfected cells were counted and inoculated into 96-well plates at a density of 1×10^4 cells/well. Five replicate wells were set up for each group.10ul CCK-8 reagent (catalog number BS350A, Biosharp, China) was added to each well regularly every day, and then incubated in the incubator for 1h. The optical density (OD) at 450nm was measured with an enzyme marker for 5 days. The experiments were repeated thrice.

Scratch Healing Assay

Cells in the logarithmic growth phase were inoculated into 6-well plates and transfected after cell attachment. After waiting for the cell density to reach 100%, the cells were scratched using a 200ul tip and the scratch healing was observed under the microscope at 0, 36, and 72 hours. The experiments were repeated thrice.

Transwell Invasion and Migration Assay

To assess the ability of cell invasion and migration, transwell chambers (catalog number 14341; LABSELECT) with and without matrix gel (catalog number 356234; Corning) were used. Take 200ul of cells resuspended with serum-free medium into the upper chamber and add 500ul of DMEM containing 10% FBS to the lower chamber. The cells were incubated at 37 °C for 48h, fixed with 4% paraformaldehyde for 20min, and stained with 0.1% crystal violet. Finally, three images were taken using a microscope for counting.

Nude Mouse Xenograft Model

The sequence of SLC35A2 mRNA (5′-CAGUAUGUUGCCAUCUA-3′) was cloned into the expression vector pGCsi-SLC35A2shRNA. The structure was modified to a short hairpin RNA (shSLC35A2): 5′-CCGGCAGTATGTTGCCA TCTCTATTCAAGAGATAGAGATGGCAACATACTTTTTG-3′ after verifying the knockdown efficiency in MCF7 cells. Viral vectors were obtained according to the viral transfection method of Liu et al.[6] MCF7 cells were cultured in culture flasks containing DMEM complete medium. Transfection efficiency was observed under a fluorescence microscope 110 hours after lentiviral transduction of shRNA-SLC35A2 or control virus. The cells were then cultured for another 130 h before implantation into nude mice. Twelve 4-week-old female BALB / c nude mice were purchased from Hangzhou Ziyuan Laboratory Animal Science and Technology Co. Ltd (China), and they were randomly divided into two groups (n = 6). MCF7 cells (5×10^6/mouse) were injected into the right axilla of nude mice. Nude mice were weighed every 3 days and tumor size was measured with calipers. Tumor growth curves were plotted according to the measurement formula: volume $=\left(\text{longdiameter} \times \text{shortdiameter}^2\right)/2$. After 3 weeks, executed the mice and then took pictures of the mice's appearance, and the tumors were carefully stripped and weighed, and photographed. The animal study was approved by the Laboratory Animal Ethics Committee of Anhui Medical University (approval number: LLSC20231253).

Results

SLC35A2 Expression in Pan-Cancer

The difference in SLC35A2 mRNA expression between all TCGA tumors and adjacent normal tissues was examined using the Xiantao website. The findings revealed that SLC35A2 was highly expressed in 16 cancers, including BLCA, LUSC, LIHC, STAD, BRCA, CHOL, COAD, ESCA, READ, HNSC, LUAD, PRAD, UCEC ($p < 0.001$), GBM ($p < 0.01$), CESC, PAAD ($p < 0.05$). Nevertheless, compared with adjacent normal tissue, KICH ($p < 0.01$) and KIRC ($p < 0.001$) both had low levels of SLC35A2 expression. It is noteworthy that SLC35A2 is not differentially expressed in only a few tumor types (such as PCPG, KIRP, SARC, SKCM, THCA, and THYM) (Figure 1A). Furthermore, because the Xiantao lacks normal controls for certain tumors, we used GTEx normal tissues as controls to assess the distinction in SLC35A2 expression between pan-cancer and normal tissues (Figure 1B, UVM and MESO without normal tissue

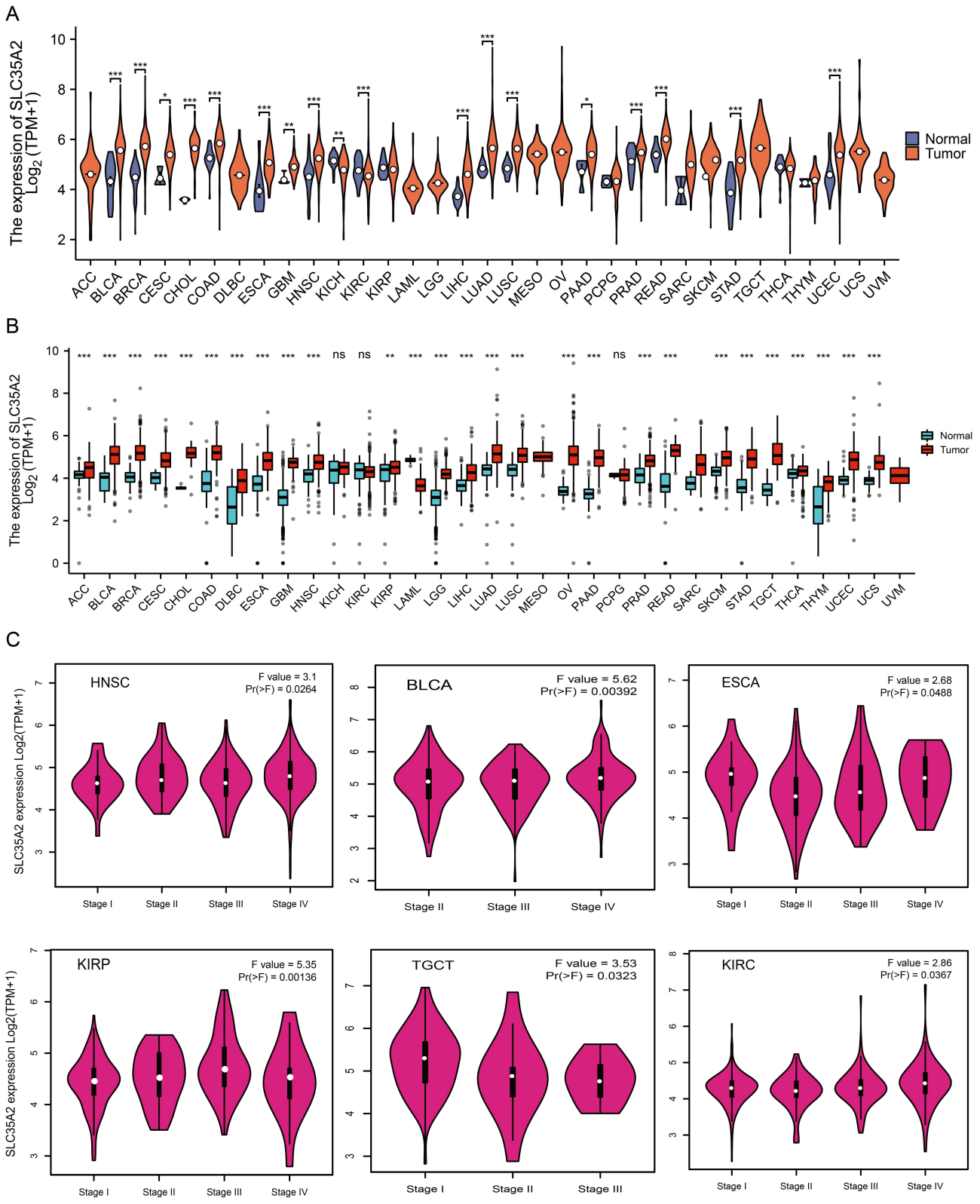

Figure 1 Differential expression analysis of SLC35A2 in pan-cancer. (**A**) The expression level of SLC35A2 in the TCGA tumor and adjacent normal tissues was visualized by Xiantao. (**B**) SLC35A2 expression levels in tumor and adjacent normal tissues from TCGA and GTEx databases, and normal tissues from GTEx database were included as controls. (**C**) Evaluate the correlation between the expression of SLC35A2 and the pathological stages of HNSC, BLCA, ESCA, KIRP, TGCT, and KIRC by using the GEPIA2. (*p < 0.05, **p < 0.01, ***p < 0.001).

controls). SLC35A2 expression in the PCPG groups was the same as that in the Xiantao, and there was no significant difference. The expression of SLC35A2 in LAML was significantly lower than that in the normal group, and the difference was statistically significant ($p < 0.001$). We found that SLC35A2 expression was significantly correlated with tumor stage in HNSC, TGCT, BLCA, ESCA, KIRP, and KIRC using the "pathological staging map" module of GEPIA2 (Figure 1C, $p < 0.05$).

Prognosis and Diagnosis Value of SLC35A2 in Pan-Cancer

To explore the possible prognosis value of SLC35A2, we utilized GEPIA2 to look at the link between SLC35A2 expression and the prognosis of various cancer patients. High SLC35A2 expression was relevant to poor OS in BRCA ($p = 2.8e-05$), PAAD ($p = 0.017$), LGG ($p = 1.1e-05$), LIHC ($p = 0.0038$), LUAD ($p = 0.0054$), and UVM ($p = 0.0013$) (Figure 2A). High SLC35A2 expression was associated with a poor prognosis for LGG, LIHC, and UVM, according to the DFS survival curve (Figure 2B). We use the Kaplan-Meier plotter to validate the relationship between SLC35A2 and OS (Supplementary Figure S1). High SLC35A2 expression was linked to a worse prognosis in the above-mentioned cancers, and the findings of these two databases were almost identical. Following that, we used univariate Cox regression analysis of the relationship between SLC35A2 expression and OS in multiple kinds of cancer. As shown in the forest plot, SLC35A2 expression was positively correlated with the hazard ratio of OS for BRCA, PAAD, COAD, LGG, LIHC, LUAD, and UVM, indicating that SLC35A2 is a risk factor for patients with the above cancers (Figure 2C). These results suggest that elevated SLC35A2 expression is a danger factor for OS/DFS and possibly a promising prognostic biomarker for patients with a variety of cancers.

The area under the ROC curve (AUC) was greater than 0.9 in BLCA, BRCA, PAAD, COAD, ESCA, LAML, LGG, GBM, OV, READ, STAD, TGCT, CESC, and UCS, indicating that tumor tissues could be accurately distinguished from normal tissues at different SLC35A2 expression levels and that SLC35A2 may be a potential diagnostic marker (Supplementary Figure S2).

Expression of SLC35A2 Correlates with Immune and Molecular Subtypes of Cancer

Next, SLC35A2 expression was analyzed in relation to cancer immunity and molecular subtypes through the TISIDB website. The findings demonstrated a relationship between several immunological subtypes and the expression of SLC35A2 in PAAD, LGG, BRCA, KIRC, LUAD, and STAD (Supplementary Figure S3A). Moreover, SLC35A2 expression varies among several molecular subtypes of a particular cancer type (Supplementary Figure S3B). Using BRCA as an illustration, SLC35A2 is highly expressed in the C2 type in the grouping of immune subtypes. In molecular subtype grouping, SLC35A2 is highly expressed in Her2 molecular subtype.

SLC35A2 Expression and Tumor Microenvironment

Based on multiple immune prediction techniques, we used the TIMER2.0 database in this study to investigate the link between abnormal SLC35A2 expression and immune cell infiltration. It was discovered that myeloid-derived suppressor cells (MDSC) infiltration was associated with elevated SLC35A2 expression in 17 cancer types (Figure 3A). As a result, we concentrated on MDSC in TME. SLC35A2 expression in LIHC, LUAD, STAD, HNSC, PAAD, and BRCA was substantially linked with the degree of MDSC infiltration, as shown in Figure 3B. We also looked at the connection between SLC35A2 expression, MDSC infiltration levels, and the prognosis of various tumor patients using the TCGA dataset from TIMER2.0. We concluded that patients with high MDSC infiltration and high SLC35A2 expression had a poor prognosis (Supplementary Figure S4).

Moreover, we found a link between SLC35A2 expression and ferroptosis-related molecules and immune checkpoints. In this analysis, the majority of malignancies' SLC35A2 expression was tightly associated with molecules related to ferroptosis (Supplementary Figure S5A). SLC35A2 expression was positively connected with several immune checkpoints in KIRP, UVM, LIHC, OV, PCPG, and LGG, but negatively correlated with immune checkpoints in CHOL, COAD, LUSC, and LUAD. Notably, almost all malignancies exhibit a positive correlation between SLC35A2 and CD276 (Supplementary Figure S5B). To understand the significance of SLC35A2 in the TME immunological mechanism, we analyzed the correlation between SLC35A2 expression and TMB and MSI. SLC35A2 was positively correlated with TMB in PAAD and THYM (Supplementary Figure S5C). SLC35A2 was positively correlated with MSI expression in KIRC, and DLBC was negatively correlated (Supplementary Figure S5D).

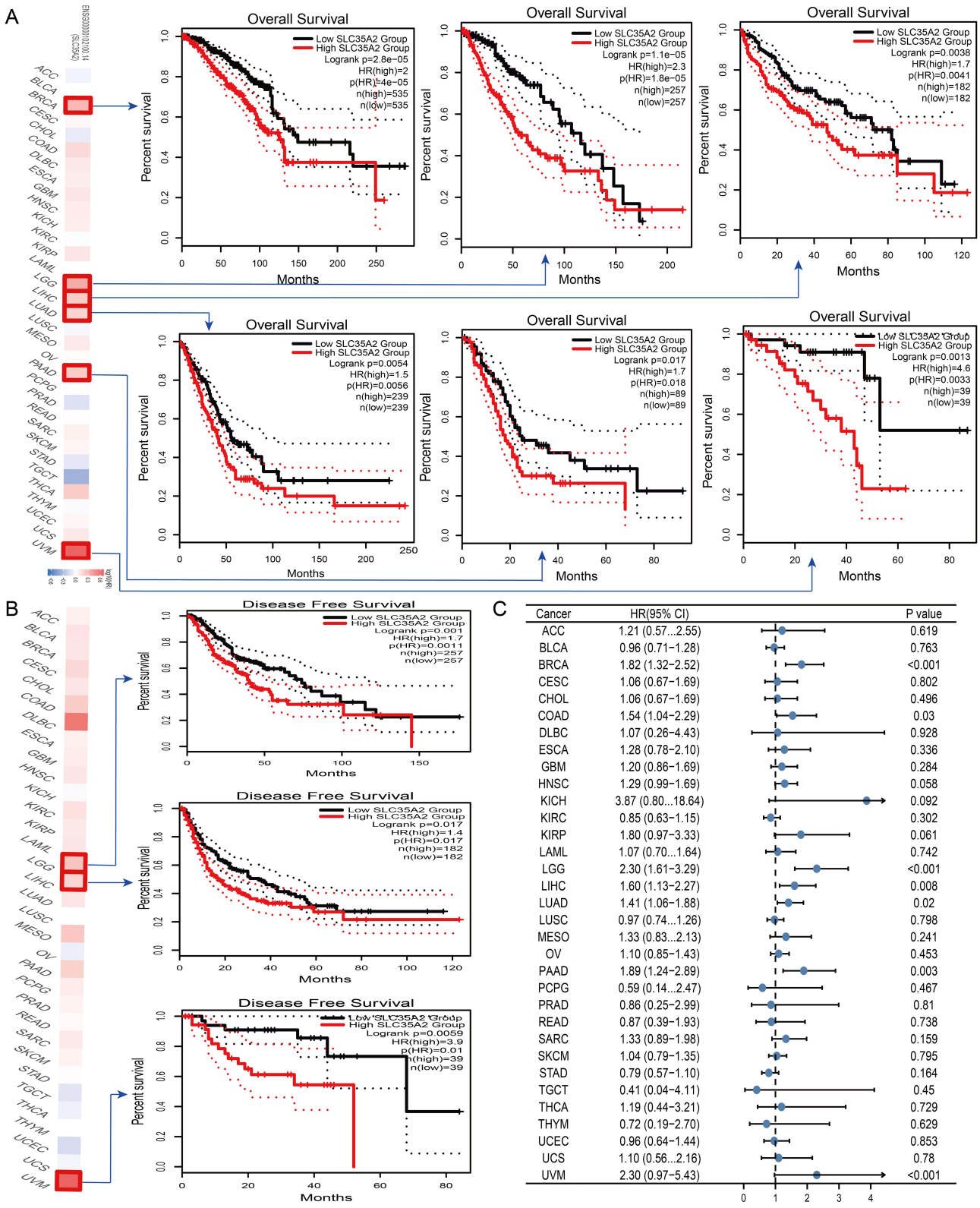

Figure 2 Relationship between SLC35A2 gene expression and prognosis of cancer. GEPIA2 was used to evaluate the relationship between SLC35A2 gene expression and OS (**A**), and DFS (**B**) in all TCGA tumors. (**C**) Using the data of the TCGA database, the survival probability of SLC35A2 was generated by univariate Cox regression analysis. HR < 1: Low-risk cancer type; HR > 1: High-risk cancer type.

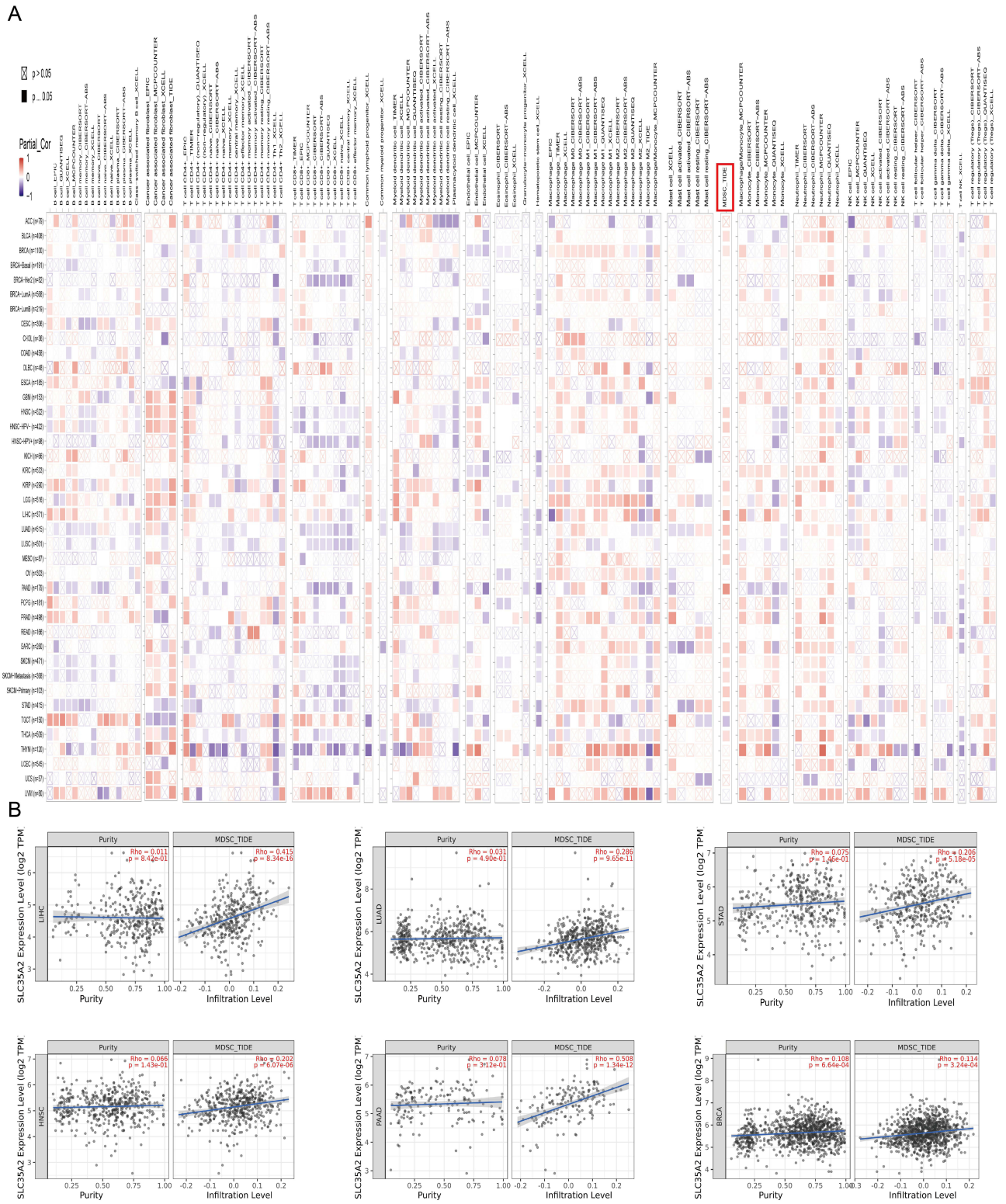

Figure 3 Correlation analysis between SLC35A2 expression and immune cell infiltration. (**A**) The thermogram represents the relationship between various immune cells and the expression of the SLC35A2 gene in all cancers. (**B**) The scatter plot represents the relationship between MDSC infiltration and SLC35A2 gene expression in LIHC, LUAD, STAD, HNSC, PAAD, and BRCA.

Enrichment Analysis of SLC35A2-Related Genes

We screened proteins that interact with SLC35A2, explored genes that are associated with SLC35A2 expression, and performed pathway enrichment analysis to learn more about the molecular mechanism of SLC35A2 in cancer. Using the

STRING online tool, we identified 46 proteins that bind to SLC35A2, which were supported by experiments, databases, and co-expression. Figure 4A depicts the 46 proteins' interaction networks. Then, the top 100 genes associated with SLC35A2 expression were obtained by combining all of the TCGA tumor expression data using the GEPIA2 tool, and the top five genes were selected for the SLC35A2 correlation scatter plot. SLC35A2 expression had a relatively strong positive correlation with the expression of TIMM17B (R = 0.64), CCDC120 (R = 0.59), PRICRLE3 (R = 0.57), OTUD5 (R = 0.55), and FTSJ1 (R = 0.52) (Figure 4B). Seven individuals shared across the two groups in the intersection analysis were identified: DDOST, DPAGT1, RPN1, RPN2, SEC61A1, STT3A, and SURF4 (Figure 4C). We then used a thermogram to express the correlation between these seven genes and SLC35A2 in pan-cancer. The seven genes indicated above and SLC35A2 have a significant positive relationship in the majority of tumor types (Figure 4D). Also, for KEGG and GO enrichment analysis, we pooled two data sets. Then, gene ontology chord and bubble diagrams were applied to bioinformatics to visualize the enrichment results. These genes were primarily associated with the biological processes of "protein glycosylation", "macromolecule glycosylation", and "protein N-linked glycosylation via asparagine", according to GO enrichment analysis (Figure 4E). KEGG pathway analysis further showed that SLC35A2 may participate in tumorigenesis through "n-glycan biosynthesis", "protein processing in endoplasmic reticulum", and "diverse types of n-glycan biosynthesis" (Figure 4F).

Correlation of SLC35A2 with Clinical Features of Breast Cancer

Based on the TCGA-breast cancer data set, Supplementary Table S2 shows the correlation between the clinicopathological traits of breast cancer patients and the level of SLC35A2 expression. The expression level of SLC35A2 is related to T stage, N stage, age, PR (Progesterone Receptor) status, ER (Estrogen Receptor) status, PAM50 status, and OS. We found that SLC35A2 expression in breast cancer was inversely correlated with histological type, ER status, and PR status, and positively related to pathological stage, age, and PAM50 status (Supplementary Table S3).

Prognostic Value of SLC35A2 in Breast Cancer

The multivariate Cox regression approach was used to assess SLC35A2's prognostic significance in breast cancer. The multivariate Cox regression forest map revealed that N3, Age > 60, ER-positive, PAM50-HER2, post-menopausal status, and SLC35A2 were independent prognostic factors for OS ($p < 0.05$) (Figure 5A). Furthermore, we created a nomogram according to independent prognosis factors of OS to promote the use of SLC35A2 in clinical evaluation (Figure 5B). By the calibration curve, we simultaneously assessed the precision of the prognostic evaluation model for breast cancer patients at 1, 3, and 5 years. The nomogram's C-index is 0.801 (95% CI = 0.752–0.849), demonstrating the model's good ability to predict OS in breast cancer patients (Figure 5C). Subsequently, we assess the SLC35A2 expression and nomogram model's discriminant power using a time-dependent ROC curve. The findings demonstrated that SLC35A2 performed well in prognosis evaluation for breast cancer. In addition, the AUC values at one year, three years, and five years were all more than 0.6 (Figure 5D). These findings demonstrate the suitability of the nomograms we constructed.

Based on the prognosis of SLC35A2 in breast cancer, to verify the predictive value of SLC35A2 in clinical subgroups, we examined the association of SLC35A2 expression with OS in each subgroup according to different clinical characteristics. The results showed that patients with high SLC35A2 expression had a significantly worse prognosis than those with low SLC35A2 levels in the following subgroups: age >60 years, M0, N0, T1, ER-positive, PR-positive, Her2-positive, LumA and LumB, stage I–II, and non-radiotherapy subgroups ($p < 0.05$) (Figure 6).

Validation of SLC35A2 in Breast Cancer

First, we researched the differences in SLC35A2 expression in breast cancer tissues. Both paired and unpaired analyses from Figure 7A and B showed that SLC35A2 was overexpressed in breast cancer tissues compared to normal tissues. We used an RT-qPCR technique to measure the levels of SLC35A2 mRNA expression in the three breast cancer cell lines MCF7, MDA-MB-231, and BT474. SLC35A2 mRNA expression was more prominent in breast cancer cells than in

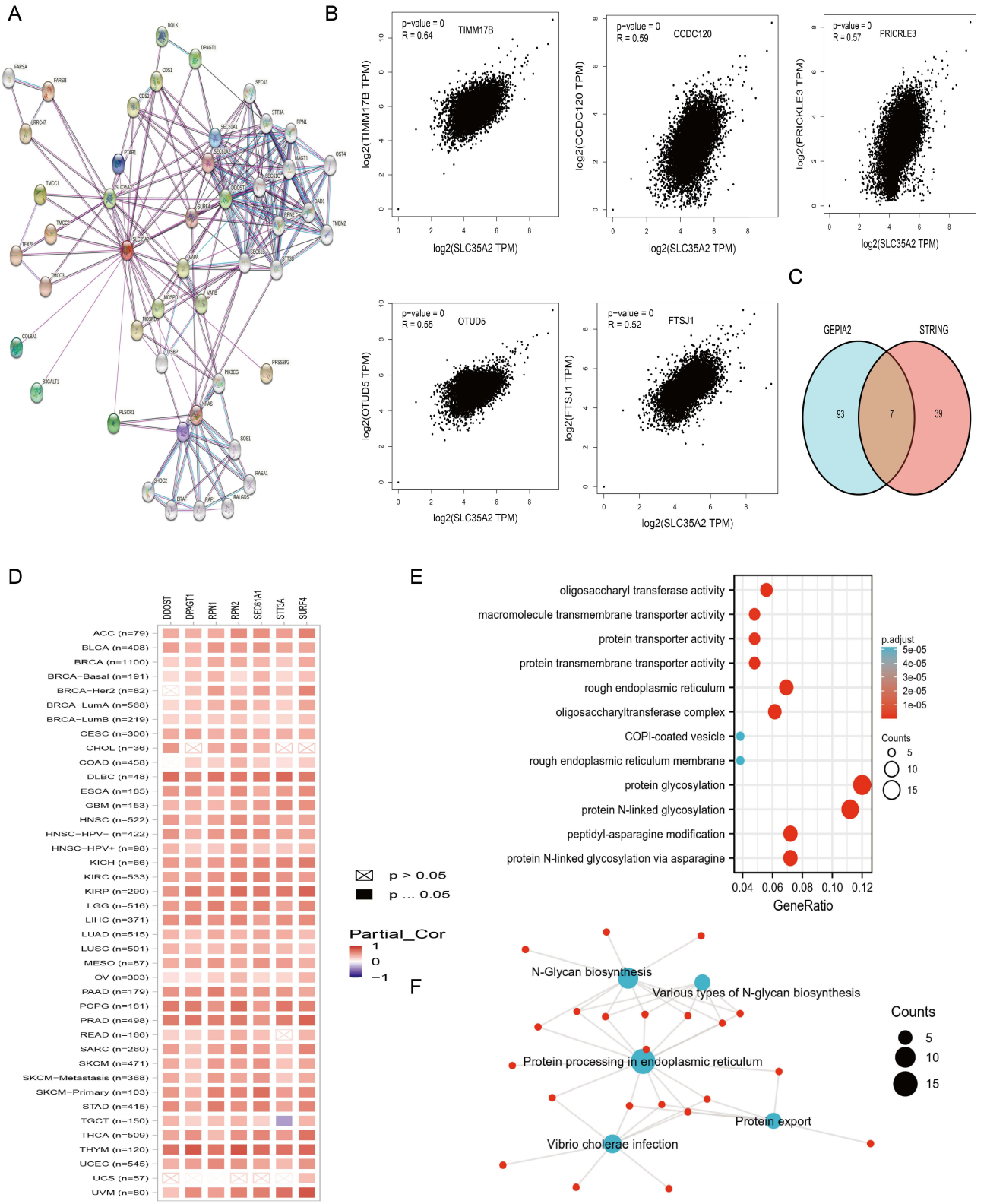

Figure 4 Enrichment analysis of SLC35A2-related genes. (**A**) SLC35A2 protein interaction network diagram. (**B**) The scatter plot of SLC35A2-related top 5 genes. (**C**) Cross-analysis of SLC35A2-related genes and SLC35A2-binding genes. (**D**) The expression of correlation between cross-genes and SLC35A2 in pan-cancer. GO analysis (**E**) and KEGG enrichment analysis (**F**) based on SLC35A2-related and SLC35A2-binding genes.

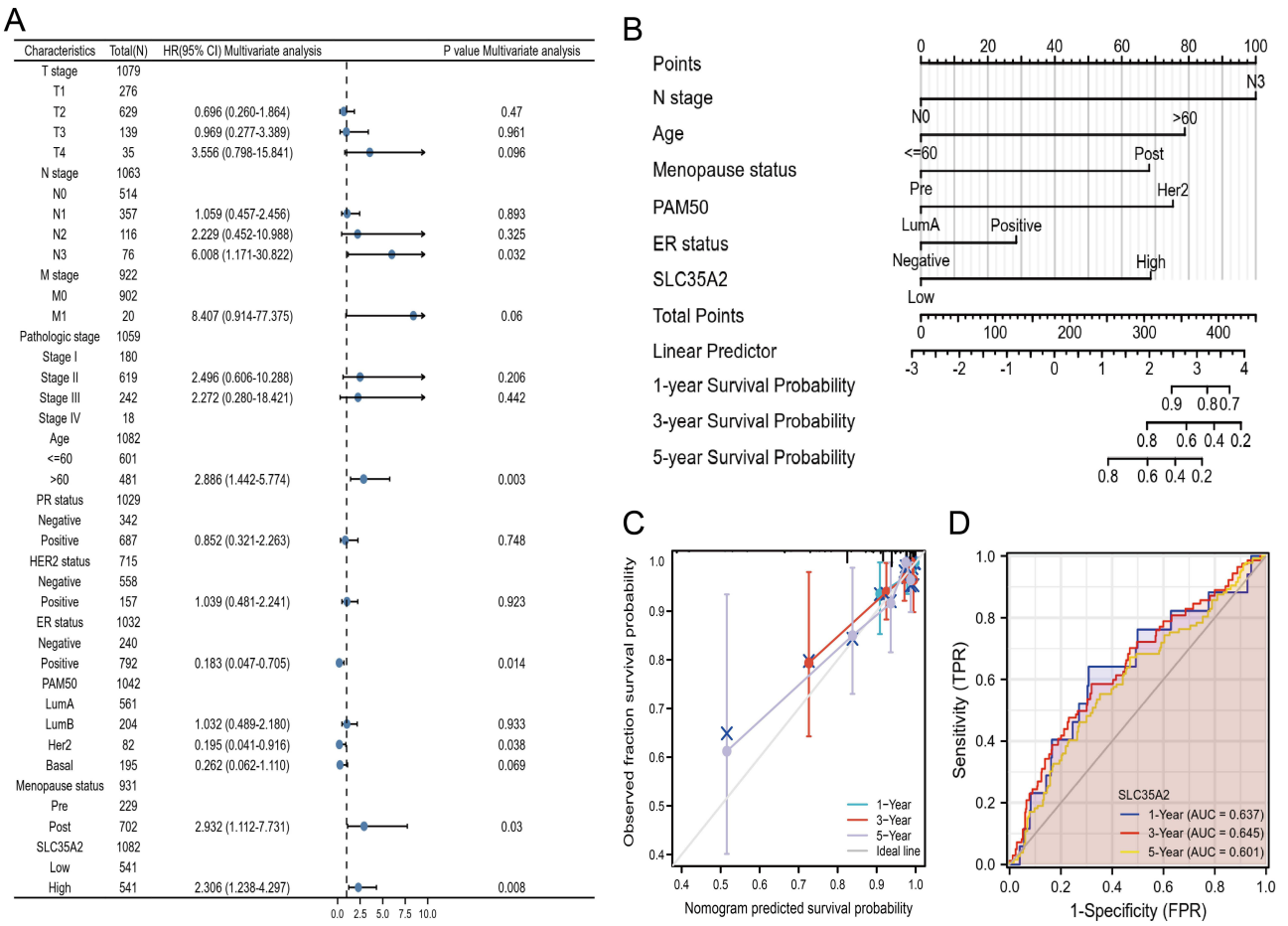

Figure 5 Prognostic modeling of SLC35A2 in breast cancer. (**A**) OS forest plot based on multivariate Cox analysis. (**B**) Nomograms for predicting the OS of 1, 3, 5 years for breast cancer patients. (**C**) The calibration curve of the nomogram for predicting the OS of breast cancer patients at one year, three years, and five years. (**D**) Time-dependent ROC curve.

normal cells (Figure 7C). By Western blot and IHC experiments, we further verified that breast cancer cells and tissues had significantly greater levels of SLC35A2 protein expression than normal breast cells or tissues (Figure 7D–F).

Effect of Knockdown of SLC35A2 on Proliferation, Invasion, Migration, and EMT of Breast Cancer Cells

Four SLC35A2 expression inhibitory siRNAs were transfected into MCF7 cells and tested for inhibition efficiency. RT-qPCR results showed that siSLC35A2-3 and siSLC35A2-4 significantly inhibited the expression of the SLC35A2 gene compared to the control (Figure 8A). Western blotting revealed that these two siRNAs greatly reduced the expression of SLC35A2 protein in the cells (Figure 8B). The CCK8 results suggested that knockdown of SLC35A2 inhibits the proliferation of MCF7 cells, see Figure 8C. Scratch assay displayed that knockdown of SLC35A2 expression suppressed the migration of MCF7 in breast cancer cells ($p < 0.001$) (Figure 8D and E). We then explored the effect of knocking down the SLC35A2 gene on the expression of EMT pathway-related proteins. E-cadherin protein expression was higher and N-cadherin expression was lower in the experimental group when compared to the control group, indicating that SLC35A2 knockdown might prevent EMT in MCF7 cells (Figure 8F). Transwell assay results showed that knockdown of the SLC35A2 gene resulted in diminished cell invasion and migration (Figure 8G).

SLC35A2 Knockdown Inhibits Tumor Growth in vivo

By analyzing the results of the above experiments, we initially concluded that SLC35A2 has a role in promoting tumor growth. To further investigate the role of SLC35A2 in vivo, we performed in vivo experiments to verify the effect of

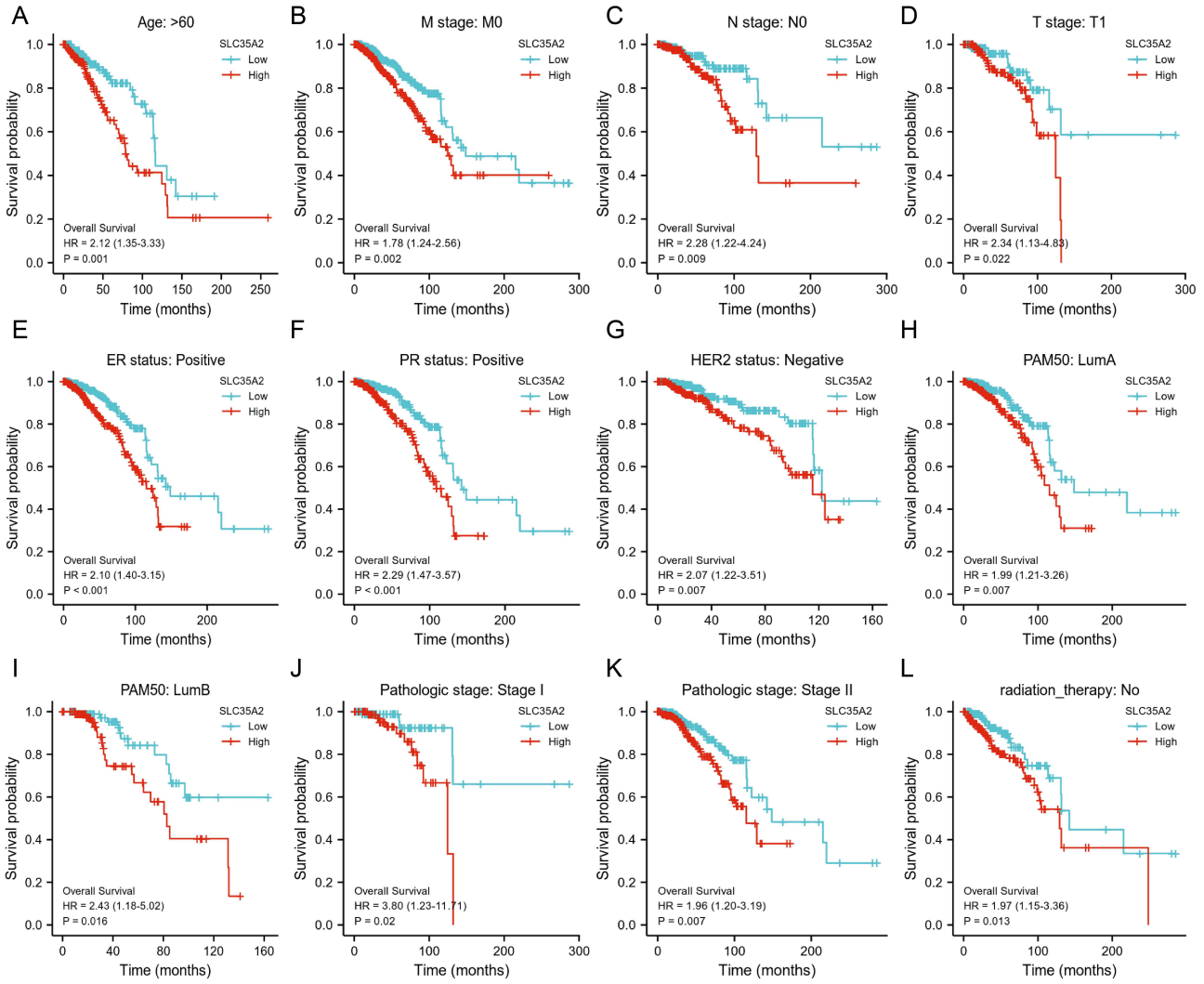

Figure 6 Kaplan-Meier plotter was used to evaluate the relationship between the expression level of SLC35A2 and the OS of breast cancer patients in different clinical subgroups. (**A**–**L**) OS curves for age > 60 years, M0, N0, T1, ER-positive, PR-positive, HER2-positive, LumA, LumB, pathological stage I–II and no radiotherapy subgroups in breast cancer patients with high SLC35A2 expression and low SLC35A2 expression.

SLC35A2 knockdown on tumor growth in nude mice in vivo. We established an axillary graft tumor model by subcutaneous injection of tumor cells into BALB/c nude mice, and tumor size was measured periodically (Figure 9A and B). The SLC35A2 knockdown group's tumor weight and size were considerably lower than those of the control group (Figure 9C and D).

Discussion

According to the results of our pan-cancer analysis, SLC35A2 is aberrantly expressed in a range of malignancies, but until now, most of the research on SLC35A2 has focused on neurological diseases and less on cancer. Therefore, a thorough analysis of SLC35A2 in the context of pan-cancer is crucial. We used multiple databases to determine the expression levels of SLC35A2 in normal and malignant tissues and cells. The findings demonstrate that SLC35A2 expression was significantly higher in 27 different cancer types. We looked into the link between high SLC35A2 expression and prognosis further. The findings are consistent with previous research, indicating that patients with high SLC35A2 expression in breast cancer[6] and hepatocellular carcinoma[5] have a poor prognosis. In many other cancer types, high SLC35A2 expression also means a worse prognosis. Additionally, in HNSC, BLCA, ESCA, KIRP, TGCT, and KIRC, SLC35A2 expression was substantially correlated with tumor stage. The aforementioned data suggest that

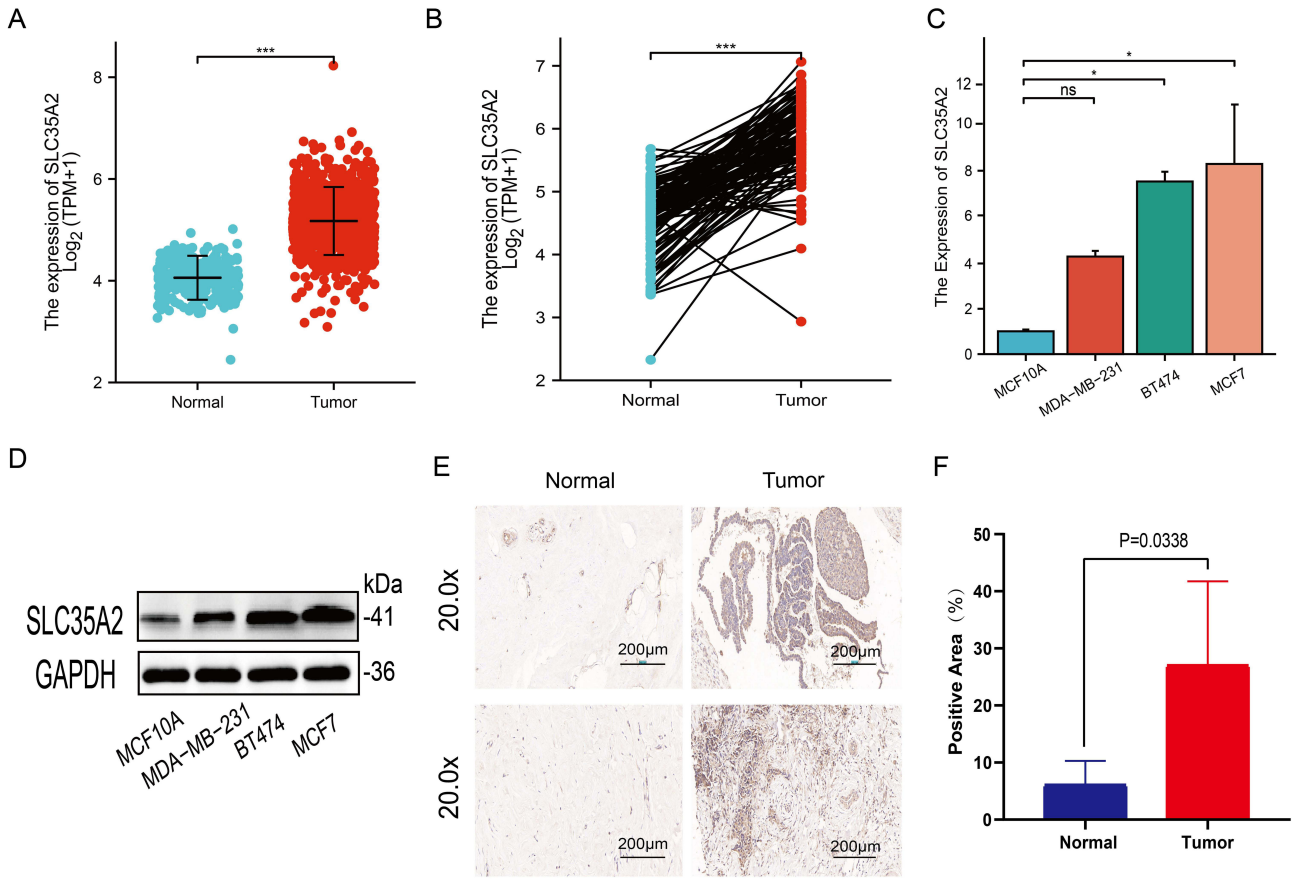

Figure 7 Verification of SLC35A2 expression in breast cancer. SLC35A2 expression in breast cancer and unmatched (**A**) /matched (**B**) normal tissues in TCGA and GTEx databases. (**C**) Relative mRNA expression of SLC35A2 in breast cancer cell lines. (**D**) Expression of SLC35A2 protein in breast cancer cell lines. (**E** and **F**) Immunohistochemical analysis of SLC35A2 in breast cancer. (*$p < 0.05$, ***$p < 0.001$).

SLC35A2 may have a carcinogenic role in promoting multiple tumors and may potentially be a prognostic biomarker. SLC35A2 has high accuracy in the diagnosis of a variety of tumors, according to ROC curve analysis. In parallel, we investigated the expression of SLC35A2 in several immune and molecular subtypes of human malignancies to determine its possible mode of action. SLC35A2 has been associated with immune and molecular subtypes in multiple cancer types, leading to the conclusion that SLC35A2 is a promising pan-cancer diagnostic biomarker and is related to immune regulation.

The complex biological environment known as the TME that surrounds tumor cells is primarily composed of immune cells, extracellular matrix, and other internal and external molecules.[17] The accumulation of abnormal metabolites in TME has become a sign of cancer.[18] An essential element of TME, tumor-infiltrating immune cells, are connected to the development and prognosis of cancer.[19–21] Despite previous studies showing that SLC35A2 affects immune cell infiltration in breast cancer, it has not been further studied in pan-cancer.[7] We performed TIMER2.0 analysis to identify that SLC35A2 expression was linked positively with MDSC infiltration in many types of cancer, which helped us better understand the relation between SLC35A2 expression in the tumor microenvironment and different immune cells. Because of its strong immunosuppressive activity, MDSC can promote tumor cell proliferation, invasion, and metastasis, and it may also accelerate the growth of tumors by triggering EMT.[22,23] As a result, we found a strong correlation between the degree of MDSC infiltration and the prognosis of individuals with different types of tumors.

A unique, iron ion-dependent form of programmed cell death known as ferroptosis plays a significant role in tumor growth. SLC35A2 was found to be positively correlated with ferroptosis-related molecules in the majority of tumors in this study. The immune checkpoint is an important regulator to maintain immune homeostasis and prevent autoimmunity.[24] We compiled a list of 44 common immune checkpoint genes and estimated their relationship to

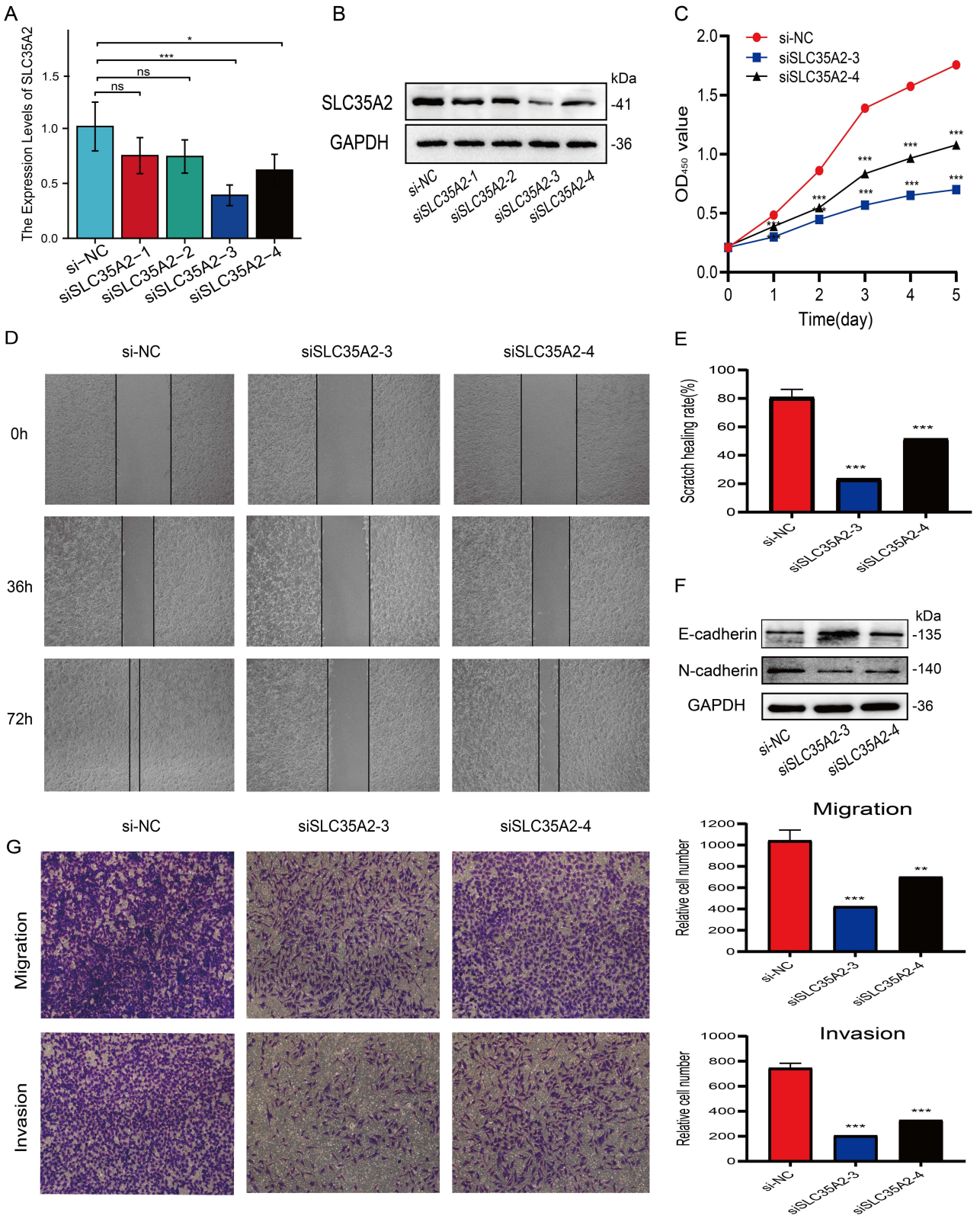

Figure 8 Effect of SLC35A2 knockdown on MCF7 cell proliferation, migration, and epithelial-mesenchymal transition (EMT). (**A**) RT-qPCR validation of mRNA levels in cells after knockdown of SLC35A2. (**B**) Western blot validation of protein levels in cells after knockdown of SLC35A2. (**C**) Proliferation activity of MCF7 cells detected by CCK-8 assay. (**D** and **E**) Cell scratch assay to detect the migration ability of MCF7 cells. (**F**) Western blot detection of the effect of knockdown of SLC35A2 on EMT protein. (**G**) Cell invasion and migration analysis using Transwell. (*$p < 0.05$, **$p < 0.01$, ***$p < 0.001$).

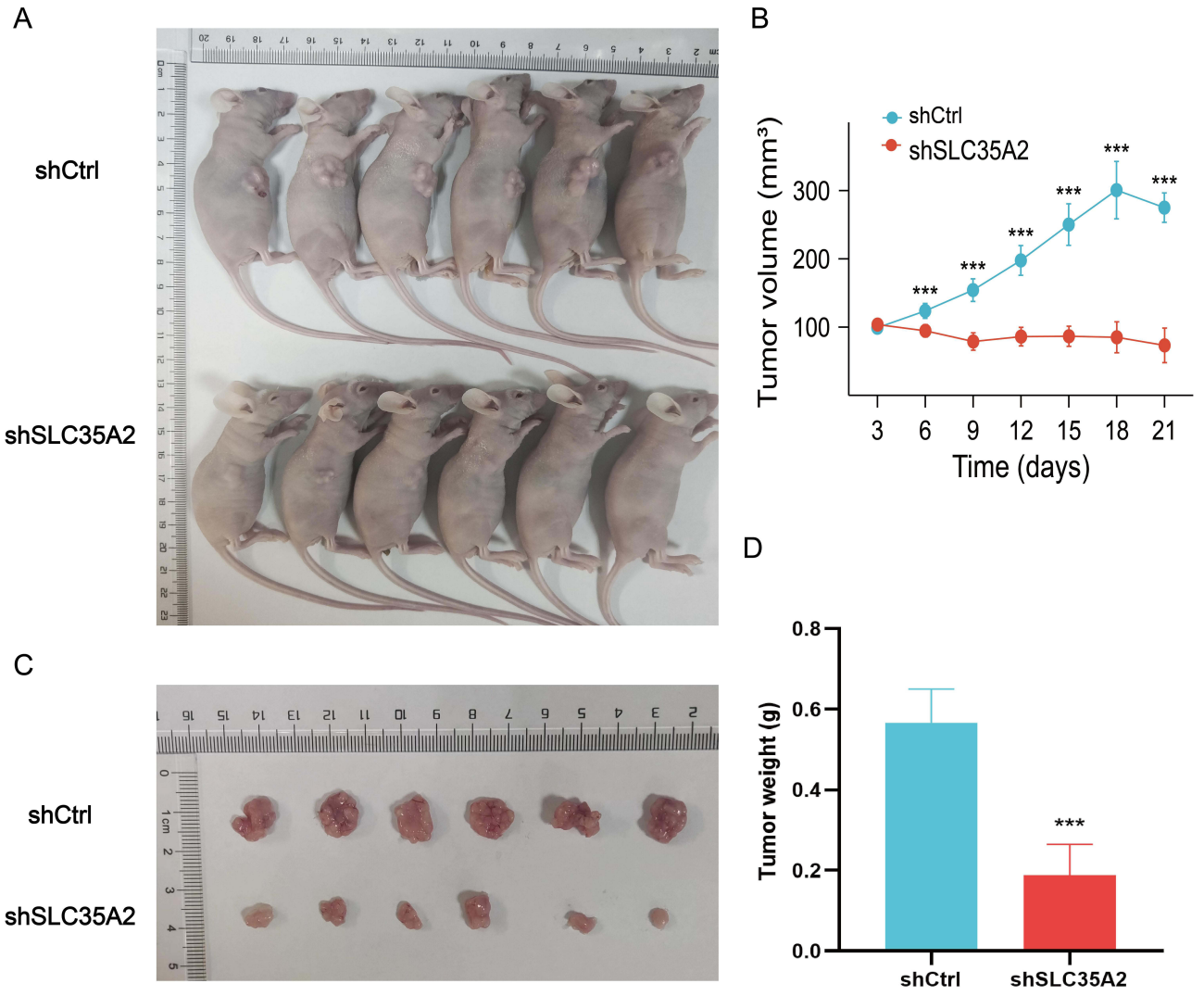

Figure 9 Knockdown of SLC35A2 inhibits breast cancer cell tumorigenesis in vivo. (**A**) The appearance of nude mice from MCF7 shCtrl and shSLC35A2 groups. (**B**) Tumor size of the two groups. (**C**) Tumor images of nude mice in the two groups. (**D**) Weight of tumors in the two groups. (***$p < 0.001$).

SLC35A2 expression. The findings of this study demonstrate a significant relationship between SLC35A2 and the immunological checkpoints in KIRP, LGG, LIHC, OV, PCPG, and UVM. TMB and MSI have been shown in tumor research to be effective prognostic markers and immunotherapy response indicators, which can guide the clinical treatment of tumor patients.[25–27] In some cancers, we noticed that SLC35A2 was also associated with TMB and MSI.

In addition, to shed light on how SLC35A2 contributes to the development of tumors, we used STRING and GEPIA2 to identify multiple proteins interacting with SLC35A2 and expression-related genes in different tumors and other tissues. In the majority of malignancies, the expression of seven genes—DDOST, DPAGT1, RPN1, RPN2, SEC61A1, STT3A, and SURF4—correlates strongly with SLC35A2 expression. It is reported that DDOST, RPN1, RPN2, and STT3A are all subunits of the oligosaccharide transferase (OST) complex, which participate in protein modification, known as N- glycosylation.[28,29] The OST subunit is a key gene-encoding protein involved in n-glycosylation in the endoplasmic reticulum lumen. The abnormality of the OST subunit can lead to the low glycosylation of protein, which in turn leads to the misfolding of protein, and finally affects the endoplasmic reticulum homeostasis. It has been established that this anomaly, known as endoplasmic reticulum stress, is connected to the aggressive behavior of tumors and the dismal prognosis of patients.[30–32] According to enrichment analysis, SLC35A2-related genes are mainly enriched in N-glycan biosynthesis, endoplasmic reticulum protein processing, protein export, and other pathways. Previous studies

have found that SLC35A2 mutations in brain cells induce epilepsy by affecting abnormal N-glycosylation in the brain.[33] SLC35A2 was recently discovered to have a crucial function in malignancies for the first time; Specifically, SLC35A2 promotes hepatocellular carcinoma metastasis by regulating cellular glycosylation modifications.[5] These findings verify the results of our gene enrichment analysis. One of the protein networks linked to cancer is the SLC35A2 network. Its role in cancer may be further investigated to help develop new cancer therapy methods.

We discovered that breast cancer patients who had elevated SLC35A2 expression had a worse outcome by examining the clinical information of patients in the TCGA database. We further investigated the relationship between SLC35A2 expression and clinicopathological staging and constructed a nomogram to facilitate the application of SLC35A2 in the prognostic assessment of breast cancer. The results indicate that SLC35A2 expression correlates with several clinicopathological features and the constructed nomogram are appropriate. We also found that in breast cancer patients, age >60 years, M0, N0, T1, ER-positive, PR-positive, Her2-positive, luminal A and luminal B, stage I–II and subgroups not treated with radiation, subgroups with high SLC35A2 expression had worse OS.

We validated the accuracy and reliability of SLC35A2 in bioinformatics analysis of cancer by RT-qPCR, IHC, and Western blot experiments, and we hope to perform similar molecular biology validation in more cancers to follow. Previous research has demonstrated that SLC35A2 knockdown dramatically reduces breast cancer cell invasion and migration.[6] In the present study, we demonstrated that SLC35A2 knockdown markedly reduced the proliferative, invasion, and migratory capacity of breast cancer cells. In addition, an in vivo xenograft model revealed that SLC35A2 knockdown MCF7 cells exhibited slower growth, which confirmed the in vitro findings. EMT is the biological process through which epithelial cells undergo a specific process to transform into cells with a mesenchymal phenotype. EMT is crucial for the development and metastasis of cancer.[34–36] The research findings indicated that the knockdown of SLC35A2 markedly increased the expression of E-cadherin proteins and decreased the expression of N-cadherin proteins. E-cadherin and N-cadherin, as EMT markers, suggest that the reduction of SLC35A2 led to the inhibition of proliferation and migration of breast cancer cells through the inhibition of the EMT process, but its involvement and regulation of this process need to be further investigated.

Even though we integrated information about SLC35A2 in pan-cancer from multiple databases, this research has several limitations. On the one hand, the sample size of some uncommon tumor types is relatively small, so it is necessary to verify larger sample data to improve the accuracy of the analysis. On the other hand, while we think that SLC35A2 expression is connected to clinical survival and immune cell infiltration in human cancer, the specific molecular mechanism remains unknown and needs additional research.

Conclusion

In conclusion, SLC35A2 may be a promising new target for cancer therapy because its expression and immune cell infiltration in several cancer types are statistically associated with the clinical outcomes of patients. SLC35A2 expression is upregulated in breast cancer tissues and cells and can promote the proliferation, invasion, and migration of breast cancer cells, and SLC35A2 is also able to induce EMT in breast cancer cells. Knockdown of SLC35A2 inhibits breast cancer tumor progression in vivo. This study confirms that SLC35A2 acts as an oncogenic factor in breast cancer, which may provide new ideas for the study of the mechanism of breast cancer occurrence and development, and provide new clues for the prevention and treatment of breast cancer.

Data Sharing Statement

The data presented in this study are available on request from the corresponding author.

Ethics Statement

The study was conducted by the Declaration of Helsinki, informed consent was obtained from patients, and approved by the Medical Ethics Committee of the First Affiliated Hospital of Anhui Medical University (approval number: 5101389). All animal experiments were approved and conducted under the supervision of the Laboratory Animal Ethics Committee of Anhui Medical University (approval number: LLSC20231253). The use of the cell lines was approved by the Medical Ethics Committee of the First Affiliated Hospital of Anhui Medical University (approval number: 2023494).

Acknowledgments

We thank the contributors to the TCGA database and the authors involved for sharing their data in the open database.

Author Contributions

All authors made a significant contribution to the work reported, whether that is in the conception, study design, execution, acquisition of data, analysis and interpretation, or in all these areas; took part in drafting, revising or critically reviewing the article; gave final approval of the version to be published; have agreed on the journal to which the article has been submitted; and agree to be accountable for all aspects of the work.

Funding

This research was funded by the Health Commission of Anhui Province (AHWJ2022a001) and the Department of Science and Technology of Anhui Province(202204295107020016).

Disclosure

The authors declare no conflict of interest.

References

1. Quelhas D, Correia J, Jaeken J, et al. SLC35A2-CDG: novel variant and review. *Mol Genet Metab Rep*. 2021;26:100717. doi:10.1016/j.ymgmr.2021.100717
2. Yates TM, Suri M, Desurkar A, et al. SLC35A2-related congenital disorder of glycosylation: defining the phenotype. *Eur J Paediatr Neurol*. 2018;22(6):1095–1102. doi:10.1016/j.ejpn.2018.08.002
3. Bonduelle T, Hartlieb T, Baldassari S, et al. Frequent SLC35A2 brain mosaicism in mild malformation of cortical development with oligodendroglial hyperplasia in epilepsy (MOGHE). *Acta Neuropathol Commun*. 2021;9(1). doi:10.1186/s40478-020-01085-3
4. Ng BG, Sosicka P, Agadi S, et al. SLC35A2-CDG: functional characterization, expanded molecular, clinical, and biochemical phenotypes of 30 unreported individuals. *Hum Mutat*. 2019;40(7):908–925. doi:10.1002/humu.23731
5. Cheng H, Wang S, Gao D, et al. Nucleotide sugar transporter SLC35A2 is involved in promoting hepatocellular carcinoma metastasis by regulating cellular glycosylation. *Cellular Oncol*. 2022;46(2):283–297.
6. Liu C-L, Cheng S-P, Huang W-C, et al. Aberrant expression of solute carrier family 35 member A2 correlates with tumor progression in breast cancer. *In Vivo (Brooklyn)*. 2023;37(1):262–269. doi:10.21873/invivo.13076
7. Ta HD, Minh Xuan DT, Tang W-C, et al. Novel insights into the prognosis and immunological value of the SLC35A (Solute Carrier 35A) family genes in human breast cancer. *Biomedicines*. 2021;9(12):1804.
8. Koike T, Kimura N, Miyazaki K, et al. Hypoxia induces adhesion molecules on cancer cells: a missing link between Warburg effect and induction of selectin-ligand carbohydrates. *Proc Natl Acad Sci U S A*. 2004;101(28):10494.
9. Girardi E, Cesar-Razquin A, Lindinger S, et al. A widespread role for SLC transmembrane transporters in resistance to cytotoxic drugs. *Nat Chem Biol*. 2020;16(4):469–+. doi:10.1038/s41589-020-0483-3
10. Tang Z, Kang B, Li C, Chen T, Zhang Z. GEPIA2: an enhanced web server for large-scale expression profiling and interactive analysis. *Nucleic Acids Res*. 2019;47(W1):W556–W560. doi:10.1093/nar/gkz430
11. Lanczky A, Gyorffy B. Web-based survival analysis tool tailored for medical research (KMplot): development and implementation. *J Med Internet Res*. 2021;23(7):e27633. doi:10.2196/27633
12. Ru B, Wong CN, Tong Y, et al. TISIDB: an integrated repository portal for tumor-immune system interactions. *Bioinformatics*. 2019;35(20):4200–4202. doi:10.1093/bioinformatics/btz210
13. Liang J-Y, Wang D-S, Lin H-C, et al. A novel ferroptosis-related gene signature for overall survival prediction in patients with hepatocellular carcinoma. *Int J Biol Sci*. 2020;16(13):2430–2441. doi:10.7150/ijbs.45050
14. Darvin P, Toor SM, Nair VS, Elkord E. Immune checkpoint inhibitors: recent progress and potential biomarkers. *Exp Mol Med*. 2018;50. doi:10.1038/s12276-018-0076-3
15. Danilova L, Ho WJ, Zhu Q, et al. Programmed Cell Death Ligand-1 (PD-L1) and CD8 expression profiling identify an immunologic subtype of pancreatic ductal adenocarcinomas with favorable survival. *Cancer Immunol Res*. 2019;7(6):886–895. doi:10.1158/2326-6066.CIR-18-0822
16. Szklarczyk D, Gable AL, Nastou KC, et al. The STRING database in 2021: customizable protein-protein networks, and functional characterization of user-uploaded gene/measurement sets. *Nucleic Acids Res*. 2021;49(D1):D605–D612. doi:10.1093/nar/gkaa1074
17. Antonio MJ, Zhang C, Le A. Different tumor microenvironments lead to different metabolic phenotypes. *Adv Exp Med Biol*. 2021;1311:137–147.
18. Lu J, Liu P, Zhang R. A metabolic gene signature to predict breast cancer prognosis. *Front Mol Biosci*. 2022;9. doi:10.3389/fmolb.2022.900433
19. Swartz MA, Iida N, Roberts EW, et al. Tumor microenvironment complexity: emerging roles in cancer therapy. *Cancer Res*. 2012;72(10):2473–2480. doi:10.1158/0008-5472.CAN-12-0122
20. Yu L, Ding Y, Wan T, Deng T, Huang H, Liu J. Significance of CD47 and its association with tumor immune microenvironment heterogeneity in ovarian cancer. *Front Immunol*. 2021;12:768115.
21. Zhang S, Ma X, Zhu C, Liu L, Wang G, Yuan X. The role of myeloid-derived suppressor cells in patients with solid tumors: a meta-analysis. *PLoS One*. 2016;11(10):e0164514.
22. Condamine T, Ramachandran I, Youn J-I, Gabrilovich DI. Regulation of tumor metastasis by myeloid-derived suppressor cells. In: Caskey CT, editor. *Annual Review of Medicine*. Vol. 66. Annual Reviews; 2015:97–110.

23. Gabrilovich DI. Myeloid-derived suppressor cells. *Cancer Immunol Res*. 2017;5(1):3–8. doi:10.1158/2326-6066.CIR-16-0297
24. Burke KP, Patterson DG, Liang D, Sharpe AH. Immune checkpoint receptors in autoimmunity. *Curr Opin Immunol*. 2023;80:102283.
25. Galvano A, Gristina V, Malapelle U, et al. The prognostic impact of tumor mutational burden (TMB) in the first-line management of advanced non-oncogene addicted non-small-cell lung cancer (NSCLC): a systematic review and meta-analysis of randomized controlled trials. *Esmo Open*. 2021;6(3):100124. doi:10.1016/j.esmoop.2021.100124
26. van Velzen MJM, Derks S, van Grieken NCT, et al. MSI as a predictive factor for treatment outcome of gastroesophageal adenocarcinoma. *Cancer Treat Rev*. 2020;86. doi:10.1016/j.ctrv.2020.102024
27. Zhang L, Li B, Peng Y, et al. The prognostic value of TMB and the relationship between TMB and immune infiltration in head and neck squamous cell carcinoma: a gene expression-based study. *Oral Oncol*. 2020;110:104943.
28. Cherepanova N, Shrimal S, Gilmore R. N-linked glycosylation and homeostasis of the endoplasmic reticulum. *Curr Opin Cell Biol*. 2016;41:57–65. doi:10.1016/j.ceb.2016.03.021
29. Ding J, Xu J, Deng Q, et al. Knockdown of oligosaccharyltransferase subunit ribophorin 1 induces endoplasmic-reticulum-stress-dependent cell apoptosis in breast cancer. *Front Oncol*. 2021;11:722624.
30. Cubillos-Ruiz JR, Bettigole SE, Glimcher LH. Tumorigenic and immunosuppressive effects of endoplasmic reticulum stress in cancer. *Cell*. 2017;168(4):692–706. doi:10.1016/j.cell.2016.12.004
31. Wang Y, Wang K, Jin Y, Sheng X. Endoplasmic reticulum proteostasis control and gastric cancer. *Cancer Lett*. 2019;449:263–271. doi:10.1016/j.canlet.2019.01.034
32. Xu D, Liu Z, Liang M-X, et al. Endoplasmic reticulum stress targeted therapy for breast cancer. *Cell Commun Signal*. 2022;20(1). doi:10.1186/s12964-022-00964-7
33. Sim NS, Seo Y, Lim JS, et al. Brain somatic mutations in SLC3SA2 cause intractable epilepsy with aberrant N-glycosylation. *Neurology-Genetics*. 2018;4(6). doi:10.1212/NXG.0000000000000294
34. Pastushenko I, Blanpain C. EMT transition states during tumor progression and metastasis. *Trends Cell Biol*. 2019;29(3):212–226. doi:10.1016/j.tcb.2018.12.001
35. Huang Y, Hong W, Wei X. The molecular mechanisms and therapeutic strategies of EMT in tumor progression and metastasis. *J Hematol Oncol*. 2022;15(1):129.
36. Lu W, Kang Y. Epithelial-mesenchymal plasticity in cancer progression and metastasis. *Dev Cell*. 2019;49(3):361–374. doi:10.1016/j.devcel.2019.04.010